Asian Journal of Chemistry; Vol. 24, No. 12 (2012), 5485-5489

ASIAN JOURNAL OF CHEMISTRY

www.asianjournalofchemistry.co.in

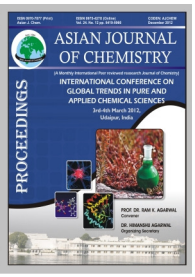

Ferrous Oxidation Catalyzed by Oxy-Nitrogen Species (NO_X)†

OZGE GOK

Department of Mining Engineering, University of Dokuz Eylul, Izmir 35160, Turkey

Corresponding author: E-mail: ozge.solak@deu.edu.tr

AJC-11674

The effect of small concentrations of nitrite (4.5 mM) on 0.1 M ferrous sulfate oxidation in a 1 M sulfuric acid under 4 atm oxygen pressure at 25, 60 and 80 ºC was investigated. A mathematical model for reaction was developed and COMSOL software was used to simulate the concentration *versus* time trajectories in parallel with previous thermodynamic and kinetics investigations on related systems. The simulations and experiments revealed that nitrous acid disproportionates to produce N_2O_3, NO and NO_2 and subsequently, these oxy-nitrogen species are all oxidized to N(V). The oxidation rate of ferrous at higher temperatures with nitrite was 32 times faster compared to that with only oxygen present. The activation energy for ferrous oxidation was found to be 34.51 kJ mol^{-1}. It is expected to identify the key reaction pathways involved in leaching processes including NOx by avoiding much of the expensive Edisonian experimentation that slows innovation.

Key Words: Autocatalysis, COMSOL, Kinetics, Mathematical modeling, Oxy-nitrogen species.

INTRODUCTION

Traditionally, the recovery of metals from sulfudic ores/concentrates involves subjecting the ores to smelting. Due to interests that include environmental aspects, there has been a world wide upsurge of interest in hydrometallurgical processes for production of metals. First attempts were made to extract valuable metals from sulfide ores using nitric acid[1-4]. In some industrial operations, sulfuric acid, with the addition of a small amount of nitric acid, was employed with air as an oxidant to leach sulfide minerals while simultaneously recovering elemental sulfur[5]. The first patented commercial process, by Sunshine Precious Metals in Idaho, used a sulfuric/dilute nitric acid mixture to leach silver- and copper-bearing ores[6]. Subsequently, nitric-acid leaching was practiced under various process acronyms such as NSL[7], NITROX[8], Arseno and REDOX[9]. More recently, the nitrogen species catalyzed pressure leaching (NSC) process was commissioned and performed successfully on an industrial scale at Sunshine precious metals[10,11]. The NSC pretreatment process was proposed as a potential alternative process that is capable of providing modest process temperatures and pressures (125-170 ºC and 6-10 atm.) as well as lower oxygen demand. It was suggested that, with the addition of small amounts of nitrite ion, the oxidation of sulfides in the presence of oxygen typically takes less than 0.5 h for a slurry containing 100 g/L of solids[12,13].

It is already known that ferrous oxidation by nitrite in an acidic electrolyte proceeds by the following reaction mechanism:

$$Fe^{2+} + HNO_2 + H^+ = Fe^{3+} + NO_{(g)} + H_2O \quad (1)$$

During oxidation, the system may contain a number of nitrogen compounds (NO_x) that have various catalytic activities. Numerous investigations have claimed that the most kinetically reactive form is nitrous acid and the dissociation products, which include nitric oxide (NO), might be the key species for the resulting autocatalysis[13]. To render the electrolyte system tractable, reaction rate data for reactions involving the five prominent, relevant oxy-nitrogen species (HNO_2, NO, NO_2, N_2O_3 and NO_3^-) and three iron species (Fe^{2+}, Fe^{3+} and $FeNO^{2+}$) were retrieved from the literature and classified in the following sections.

Autocatalysis of oxy-nitrogen species in an acidic electrolyte: The initiating reagent, HNO_2, for the catalytic effect is produced by the protonation of NO_2^- and its concentration is dependent on the hydrogen ion activity[14].

$$H^+ + NO_2^- = HNO_2;\ K = 2.51 \times 10^3\ M^{-1}\ (25\ ºC) \quad (2)$$

Thus, the disproportionation of nitrous acid takes place with the depletion of acid. The overall equation for the liquid phase decomposition of nitrous acid in the absence of oxygen is given by[15]:

$$3HNO_{2(aq)} \rightarrow H^+ + NO_3^- + 2NO_{(g)} + H_2O \quad (3)$$

†Presented at International Conference on Global Trends in Pure and Applied Chemical Sciences, 3-4 March, 2012; Udaipur, India

TABLE-1
REACTIONS IN COMSOL AND NET RATE EXPRESSIONS FOR THE Fe^{2+}- HNO_2- H_2SO_4 SYSTEM AT 25 ºC

Reaction No	Reaction	Reaction Rate-Expression	Reaction Classification
I	$2HNO_{2(aq)} = N_2O_{3(aq)} + H_2O$	$-r_{HNO2} = k_{If} C_{HNO2}^2 - k_{Ib} C_{N2O3}$	Elementary
II	$N_2O_{3(aq)} = NO_{(aq)} + NO_{2(aq)}$	$-r_{N2O3} = k_{IIf} C_{N2O3} - k_{IIb} C_{NO} C_{NO2}$	Elementary
III	$4NO_{(aq)} + O_{2(aq)} + 2H_2O \rightarrow 4HNO_{2(aq)}$	$-r_{O2} = k_{IIIf} C_{NO}^2 C_{O2}$	Elementary
IV	$2NO_{2(aq)} + H_2O = H^+ + NO_3^-{}_{(aq)} + HNO_{2(aq)}$	$-r_{NO2} = k_{IVf} C_{NO2}^2 - k_{IVb} C_{H+} C_{NO3-} C_{HNO2}$	Elementary
V	$Fe^{2+} + HNO_{2(aq)} + H^+ = Fe^{3+} + NO_{(aq)} + H_2O$	$-r_{Fe2+} = C_{Fe2+} C_{HNO2} (k_{V-1} + k_{V-2} C_{H+} + k_{V-3} C_{HNO2}/C_{NO}) - C_{Fe3+} (k_{V-4} C_{NO}/C_{H+} + k_{V-5} C_{NO} + k_{V-6} C_{HNO2}/C_{H+})$	Non-elementary
VI	$Fe^{2+} + NO_{2(aq)} + H^+ = Fe^{3+} + HNO_{2(aq)}$	$-r_{Fe2+} = k_{VI-1} (C_{Fe2+}) C_{NO2} - k_{VI-2} (C_{Fe3+}) C_{HNO2} / C_{H+}$	Non-elementary
VII	$Fe^{2+} + NO_3^- + 2H^+ = Fe^{3+} + NO_{2(aq)} + H_2O$	$-r_{Fe2+} = k_{VIIf-1} (C_{Fe2+}) C_{NO3-} - k_{VII-2} (C_{Fe3+}) C_{NO2}/C^2_{H+}$	Non-elementary
VIII	$Fe^{2+} + NO = Fe(NO)^{2+}$	$-r_{Fe2+} = k_{VIII-1} (C_{Fe2+}) C_{NO} - k_{VIII-2} (C_{FeNO2+})$	Elementary

Non-elementary reaction steps provide important information toward a more complete understanding of the regeneration process. A reaction scheme that takes into account both the steady-state absorption of NO_x gases into electrolyte and the disproportionation reactions can be adequately represented in Table-1 (Reaction I-IV)[16-18]. Based on the compiled data from the literature a number of important features of these reactions can be concluded: (i) The kinetics of HNO_2 disproportionation to $NO_{(g)}$ and $NO_{2(g)}$ have been described by a two-step, homogeneous, elementary reaction mechanism[19]. The evidence for the intermediate product, $N_2O_{3(g)}$ has been described most convincingly in the work of Bunton and Stedman[20]. They showed that nitrous acid exchanges only one oxygen atom with the solvent during the nitrosation (Reaction I). (ii) The nitrogen species with a 3+ oxidation state, N_2O_3 (anhydrous nitrous acid) is a highly soluble species with a Henry`s law solubility coefficient (25 ºC) of 0.7 M atm^{-1} and is reported to the electrolyte in higher rates. (Reaction II) (iii) The rate of homolysis of $N_2O_{3(aq)}$ to $NO_{(g)}$ and $NO_{2(g)}$ has been found to be much greater than that of hydrolysis to HNO_2[21]. (iv) The conversion of $NO_{2(g)}$ to $N_2O_{4(g)}$ is favourable at a lower temperature (20 ºC) and the dimer species is more soluble in the acidic electrolyte[22]. However, at extremely low $NO_{2(g)}$ partial pressures, the absorption of nitrogen dioxide is the predominant absorption route (reaction III, IV). (v) Nitrogen dioxide immediately reacts with water to form two oxyacids: nitric and nitrous acids[23] (reaction V). (vi) Nitrous acid is unstable in the presence of an acidic electrolyte and yields additional nitric acid and nitric oxide[24]. The nitrous acid regeneration cycle is completed by this equilibrium and reproduces one third of initial amount of nitrous acid. (vii) All of the nitrogen species that evolve in the electrolyte from the nitrite salt are oxidized to nitrate (NO_3^-) except $NO_{(g)}$. Nitric oxide gas is more likely to be in the gas phase due to its lower solubility [1.9×10^{-3} M atm^{-1} (25 ºC)], which is 15 times smaller than that of NO_2. (viii) In the oxidizing environment, nitric oxide is oxidized to NO_2 with the following trimolecular equation[25]:

$$2NO_{(g)} + O_{2(g)} \rightarrow 2NO_{2(g)}; \quad k = 28.34 \text{ atm}^{-2} \text{ s}^{-1} \qquad (4)$$

Oxidation of ferrous to ferric ion by oxy-nitrogen species: Significant effort[12,15,16] has been devoted to investigating the reaction mechanisms associated with ferrous oxidation by oxy-nitrogen species. It is understood that the reaction sequence is initiated by attack of a ferrous ion on nitrite even in the absence of oxygen. The reaction pathway is non-elementary and with nitrous acid acting as the oxidant, its rate is described by a three-rate coefficient rate equation (reaction no V, VI, VII) (Table-1).

Formation of a $FeNO^{2+}$ complex: The formation/decomposition rates of the dark green-coloured ferrous-nitric oxide complex have been measured spectrophotometrically using a temperature-jump technique[16]. This complex was found to be stable only at ambient conditions. The experiments performed at 120 ºC using several ferrous concentrations and initial ferrous/ferric concentration ratios indicated that increased initial ferrous concentrations did not adversely affect the reaction rates due to binding of nitric oxide in a ferrous-nitrosyl complex[12]. This result suggested that most of the nitrogen species were in solution, bound perhaps as $Fe(NO)^{2+}$ and that oxidation must somehow take place there and not in the gas phase. The reported reaction is elementary (reaction VIII) and rate coefficients are listed in Table-2.

TABLE-2
REACTION RATE CONSTANTS FOR THE REACTION RATE EXPRESSIONS

Reaction No	Reaction rate coefficient (25 ºC)		Equilibrium constant (25 ºC)		Ref.
I	k_{If}	$17.7 \text{ M}^{-1}\text{s}^{-1}$	K_I	$3 \times 10^{-3} \text{ M}^{-1}$	20
	k_{Ib}	$5.8\times10^3 \text{ s}^{-1}$			18
II	k_{IIf}	$1.18\times10^5 \text{ s}^{-1}$	K_{II}	1.19×10^{-4} M	21
	k_{IIb}	$1.1\times10^9 \text{ M}^{-1} \text{ s}^{-1}$			
III	k_{IIIf}	$2.1 \times 10^6 \text{ M}^{-2} \text{ s}^{-1}$	K_{III}	Irreversible	25
IV	k_{IVf}	$1.7\times10^8 \text{ M}^{-1} \text{ s}^{-1}$	K_{IV}	6.3×10^9 M	26
	k_{IVb}	$2.7\times10^{-2} \text{ M}^{-2} \text{ s}^{-1}$			
V	k_{V-1}	$7.8\times10^{-3} \text{ M}^{-1}\text{s}^{-1}$	K_V	7.4×10^3 atm. M^{-1}	15
	k_{V-2}	$2.3\times10^{-1} \text{ M}^{-2}\text{s}^{-1}$			
	k_{V-3}	$7.6\times10^{-3} \text{ M}^{-1}\text{s}^{-1}$			
	k_{V-4}	$5.6\times10^{-4} \text{ s}^{-1}$			
	k_{V-5}	$1.6\times10^{-2} \text{ M}^{-1}\text{s}^{-1}$			
	k_{V-6}	$5.4\times10^{-4} \text{ M}^{-1}\text{s}^{-1}$			
VI	k_{VI-1}	$3.1\times10^4 \text{ M}^{-1} \text{ s}^{-1}$	K_{VI}	$4.70 \times 10^{-7} \text{ M}^{-1}$	15
	k_{VI-2}	$6.6\times10^{-4} \text{ s}^{-1}$			
VII	k_{VII-1}	$1.5\times10^{-4} \text{ M}^{-2} \text{ s}^{-1}$	K_{VII}	$7.1 \times 10^{-3} \text{ M}^{-2}$	15
	k_{VII-2}	$2.1\times10^{-2} \text{ M s}^{-1}$			
VIII	k_{VIII-1}	$6.2\times10^5 \text{ M}^{-1} \text{ s}^{-1}$	K_{VIII}	$4.4 \times 10^2 \text{ M}^{-1}$	16

k_f: Forward reaction; k_b: Back reaction

EXPERIMENTAL

In this study, further elucidation of the oxidation reaction mechanisms of ferrous ion in the presence of oxygen and oxy-nitrogen species was attempted. First, the concentration-time

trajectories of oxy-nitrogen and iron species are provided with a predictive model for this complex system. Second, experimental studies were conducted at elevated temperatures to determine the increasing in the oxidation effect of nitrite species. Finally, a reaction mechanism that combines the data retrieved from the simulation and experiments was proposed.

Computational approach

Choice of independent species: The literature reports many other species (NO^+, N_2O_4, NO_3^{2-}, $H_2NO_2^+$, $H_2NO_3^+$) that may be present in the electrolyte. The unambiguous characterization of the kinetic time course and elucidation of the catalytic mechanism of oxy-nitrogen species were difficult. NO^+ and N_2O_4 were assumed as dependent species due to their counterparts in solution proceed at higher rates compared with the other reactions involved and could be considered to be at equilibrium. Some of the reactions of the proposed mechanism may not be elementary reactions and they may proceed through intermediates ($H_2NO_2^+$, $H_2NO_3^+$) that were not included in the simulation. Furthermore, only the NO_3^- ion was considered in the simulation, due to insufficient proton activity ($pK_\alpha = -1.4$) to produce HNO_3. Finally, the initial Fe^{2+} is converted to Fe^{3+} according to iron mass balance. To monitor the system and limit our basic reaction scheme, ten major, kinetically independent species have been chosen. The numerical template of the independent species used in the simulation is presented below;

$$1\equiv HNO_{2(aq)},\ 2\equiv H^+,\ 3\equiv N_2O_3,\ 4\equiv NO_{(aq)},\ 5\equiv NO_{2(aq)},$$
$$6\equiv NO_3^-,\ 7\equiv O_{2(aq)},\ 8\equiv Fe^{2+},\ 9\equiv Fe^{3+},\ 10\equiv FeNO^{2+}$$

Principle reactions: Net reaction rate expressions for eight equations (Table-1) were defined. The set of rate equations was integrated numerically using a robust software module, COMSOL multiphysics 3.5-reaction engineering lab module. The program used a nonlinear least squares (NLS) algorithm implementing the Gauss-Newton method. All relevant reactions, kinetic parameters (reported at 25 ºC, Table- 2) and initial conditions were incorporated into the software to solve the ODE`s describing the concentration-time profiles (trajectories) of the species. The oxygen (O_2) partial pressure was maintained at approximately 4 atm and the proton activity was the a value commensurate with the H_2SO_4 concentration (1 M) of the electrolyte. Thus, the sulfuric acid served as an ionic strength buffer in the system. The kinetic parameters (*i.e.*, reaction rate constant, frequency factor and activation energy) were extracted for a Fe^{2+}-HNO_2-O_2 system from the laboratory experiments by COMSOL parameter estimation feature.

The experiments were initiated by introducing $NaNO_2$ salt into the electrolyte containing 0.1 M $FeSO_4$ and 1 M H_2SO_4 to provide a concentration of 4.5 mM, followed by pressurizing with oxygen to 4 atm. The temperature of the reactor was maintained at 25, 60 and 80 ºC by circulation of hot water through the water jacket. Samples of the Fe^{2+}-O_2 experiments taken every hour analyzed by titration with 1×10^{-2} M $KMnO_4$. Chemical analyses of Fe^{2+} and nitrogen species [N(III), N(V)] in the electrolyte were performed using a UV/visible spectrophotometer. Chemiluminescence gas analyzer was utilized to monitor the concentrations of nitric oxide and oxides of nitrogen ($NO_x \equiv NO + NO_2$) in the gas space of the oxygen-pressurized reactor for the ferrous oxidation experiments.

RESULTS AND DISCUSSION

Prior to conducting the experiments to provide concentration-time trajectories of the eight species, a predictive simulation was performed.

Simulation of ferrous-nitrite system: The simulation results of ferrous-nitrite solution system reveal that the Fe^{2+} and Fe^{3+} concentrations are equal after 62 min, as ferrous ions are oxidized. Ultimately, 99 % conversion of the ferrous was achieved in 36 h. Fig. 1 illustrates that the concentration of NO_3^- increases gradually as the decreasing HNO_2 concentration (0.2 mM) after 5 h. Nitrous acid reduction by ferrous ions leads to the high concentration of nitric oxide, but complexation of ferrous ions and nitric oxide limits the concentration of the free ligand. Therefore, NO_2 production is also limited. The low concentration of NO_2 in turn leads to a slower increase in the NO_3^- concentration. The nitric oxide concentration increased over a period of 1 min to a maximum concentration of 3.56×10^{-5} M, after which it decreased continuously. The concentrations of NO_2 and N_2O_3 are not included in the graph because they attain a maximum concentration of only 10^{-8} M and subsequently decrease to even smaller values (10^{-10} M). The maximum concentration of the $FeNO^{2+}$ complex is 1.5×10^{-3} M after 1 min and the complex decomposes thereafter to produce free nitric oxide.

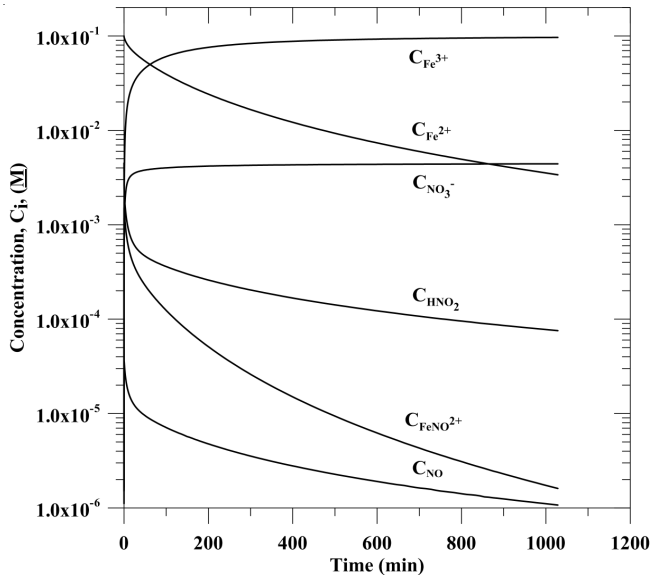

Fig. 1. Time trajectories of concentration of active species in solution obtained from simulation. Initial electrolyte concentrations: C_{FeSO_4} = 0.1 M, C_{NaNO_2} = 4.50 mM, $C_{H_2SO_4}$ = 1.0 M, ionic strength *ca.* 2.1 M. P_{O_2} *ca.* 50 psig; *ca.* 4 atm

Ferrous oxidation with oxy-nitrogen species: Initially, the ferrous oxidation rate was examined under 4 atm of O_2 pressure in the absence of nitrite to compare the oxidation effect of oxygen with oxy-nitrogen species. The elapsed time to achieve a 20 % conversion of ferrous at 25 ºC and 80 ºC was 96 h and 8 h, respectively. Fig. 2 shows straight-line plots of $1/C_{Fe2+}$ *versus* time multiplied by oxygen partial pressure, which confirms the second order rate law with respect to the ferrous ion concentration[12].

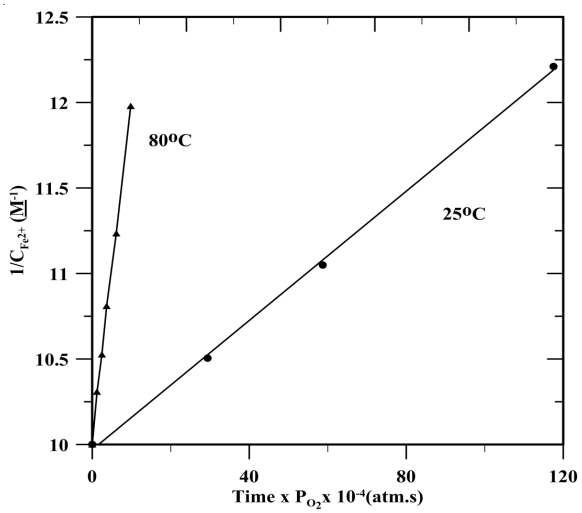

Fig. 2. Time trajectories of ferrous concentration in the absence of nitrite at 25 and 80 ºC

From the slopes of the lines presented in Fig. 2, rate constants, k_6, of 1.85×10^{-6} M^{-1} atm^{-1} s^{-1} for 25 ºC and 2.09×10^{-5} M^{-1} $atm^{-1}s^{-1}$ at 80 ºC were obtained. It is obvious that the oxidation rate of ferrous by oxygen is slow, even at higher temperatures, due to the low solubility of gaseous oxygen in electrolyte solutions. Therefore, a stronger oxidizing agent, sodium nitrite, was used to enhance the oxidation rates of ferrous at relatively lower temperatures and pressures. The experiments were conducted at 25, 60 and 80 ºC to oxidize 0.1 M Fe^{2+} with 4.5 mM $NaNO_2$ under the total oxygen pressure of 4 atm (Fig. 3). The optimum $NaNO_2$ concentration required for the oxidation of 0.1 M Fe^{2+} in 1 M H_2SO_4 at 4 atm O_2 was reported to be 4.5 mM[27]. The analysis revealed that 20 % of the ferrous is oxidized in approximately 15 min and that a 99 % conversion is realized at 17 h at a temperature of 80 ºC. It should be noted that in the presence of nitrite at 80 ºC, the rate of ferrous oxidation is 32 times higher compared to oxidation of ferrous with only O_2. The observations revealed that the ferrous-nitrosyl complex, as evident by its green-black colour, had disappeared after approximately 3 h at 25 ºC and after 1 h at 80 ºC.

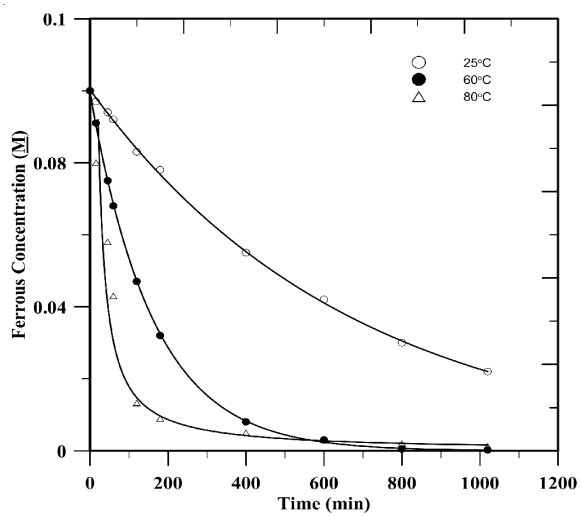

Fig. 3. Time trajectories of the ferrous concentration in the presence of nitrite at 25, 60 and 80 ºC

The kinetic data obtained from the experiment were incorporated into the COMSOL software to calculate the kinetic parameters. Rate constants of 5.23×10^{-3}, 2.27×10^{-2} and 4.59×10^{-2} $M^{-1}s^{-1}$ were obtained for 25, 60 and 80 ºC, respectively. The activation energy, E_a, was found to be 34.51 kJ mol^{-1} and the frequency factor, A, was 5.89×103 $M^{-1}s^{-1}$.

Spectrophotometric analyses (Fig. 4a-b) were conducted to monitor the oxy-nitrogen species in the electrolyte. However, the analyses had to be performed at 25 ºC due to the decomposition possibility of ferrous-nitrosyl complex. The nitrite concentration decreased at higher rates and nitrate increased gradually as observed from the simulation. This decrease was attributed to the formation of gaseous species (NO, NO_2 and NO_x), which could not be analyzed using the spectrophotometer. The oxy-nitrogen species (NO and NO_2) in the gas phase were monitored to understand the cycle of the nitrogen species in the autocatalytic process at 25 ºC.

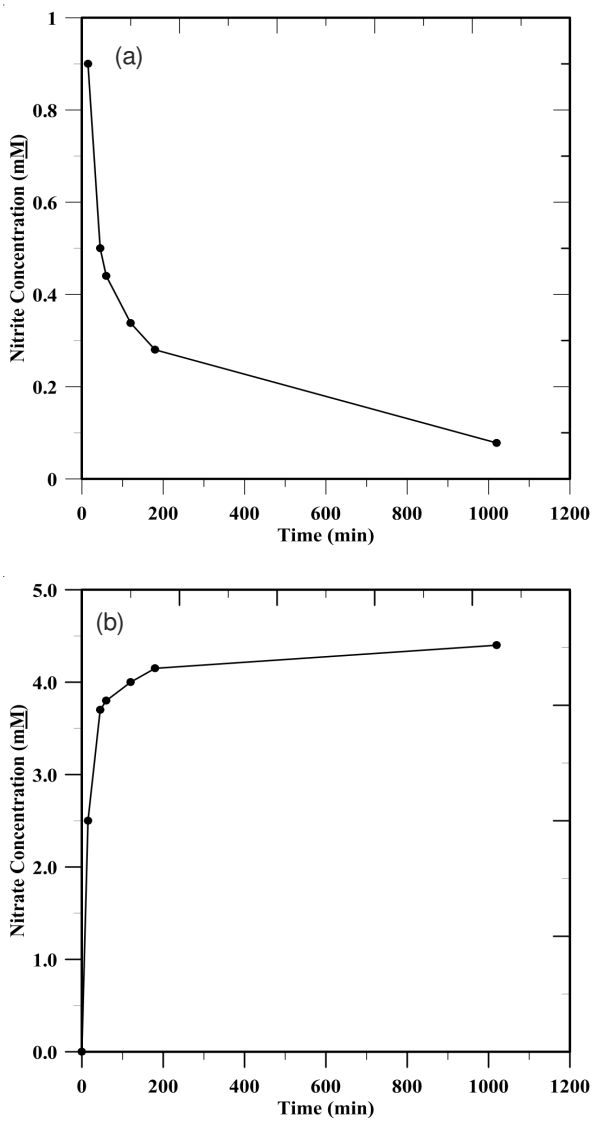

Fig. 4. Time trajectories of the concentration of (A) Nitrite and (B) Nitrate in the electrolyte

Using the chemiluminescence analyzer data presented in Fig. 5, the maximum concentrations for $NO_{(g)}$ and $NO_{2(g)}$ were 15 ppm and 25 ppm, respectively, over the course of the

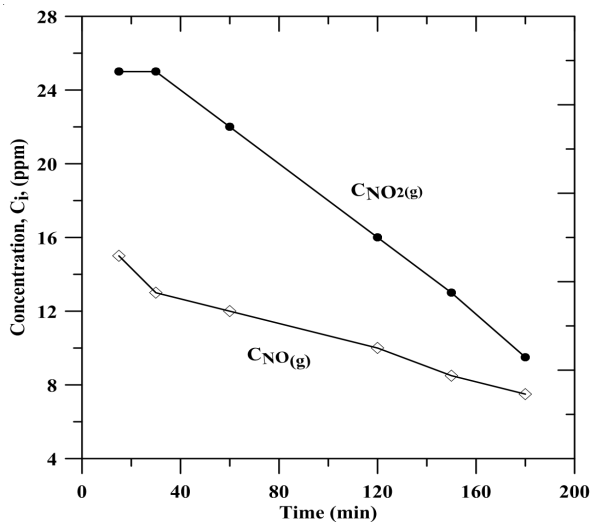

Fig. 5. Concentration profile of $NO_{(g)}$ and $NO_{2(g)}$ in the gas phase above the nitrite electrolyte at 25 ºC

reaction. Concentrations of $NO_{(g)}$ and $NO_{2(g)}$ were three orders of magnitude smaller than the initial nitrite concentration and decreased continuously. The gaseous species of nitrogen did not appear to be in equilibrium with the species in the electrolyte solution. The continuous decrease in gaseous species concentration was initially caused by the transfer of $NO_{(g)}$ from the electrolyte to the gas phase and reaction with O_2 to produce $NO_{2(g)}$. Then, $NO_{2(g)}$ immediately dissolves into the electrolyte solution and disproportionates to HNO_2 and NO_3^-.

The simulation, including the kinetic data retrieved from the literature and the results obtained from the experiments, demonstrate that the ferrous oxidation mechanism includes four main components:

I- Main reaction of Fe^{2+} oxidation:

$$Fe^{2+} + HNO_{2(aq)} + H^+ = Fe^{3+} + NO_{(aq)} + H_2O \quad (5)$$

II- Main reactions of catalyst consumption:

$$2HNO_{2(aq)} = NO_{(aq)} + NO_{2(aq)} + H_2O \quad (6)$$

$$Fe^{2+} + NO = Fe(NO)^{2+} \quad (7)$$

III- Main reactions of catalyst regeneration:

$$4NO_{(aq)} + O_{2(aq)} + 2H_2O \rightarrow 4HNO_{2(aq)} \quad (8)$$

$$Fe^{2+} + NO_{2(aq)} + H^+ = Fe^{3+} + HNO_{2(aq)} \quad (9)$$

IV- Side reaction that converts the catalyst to nitrate:

$$2NO_{2(aq)} + H_2O = H^+ + NO_3^- + HNO_{2(aq)} \quad (10)$$

According to the proposed mechanism, once the nitrite has been added to the solution containing ferrous ions, it produces nitrous acid due to the high proton activity. The attack of the ferrous ion on the catalytic nitrous acid to produce nitric oxide species initiates the reaction sequence and the ferrous-nitrosyl complex is produced. Surprisingly, the ferrous-nitrosyl complex does not adversely affect the reaction rates. In contrast, it works as a host species that increases the diffusivity of nitric oxide species into the solution. The nitric oxide species can then be oxidized to NO_2. Finally, as presented in Fig. 6, NO_2 disproportionates to HNO_2 and NO_3^- when oxygen is present in the electrolyte system, to increase the oxidation potential of the

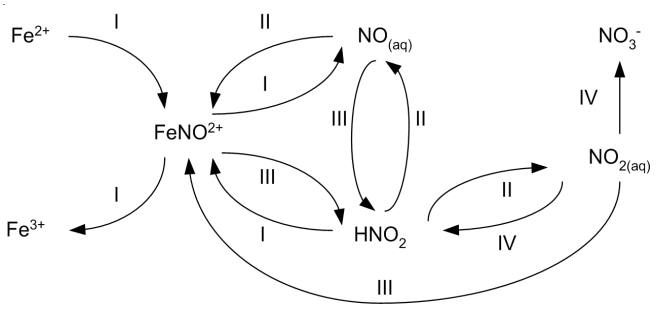

Fig. 6. Proposed catalytic route for ferrous oxidation with nitrous Acid

ferrous ions. The slow initial build-up of Fe^{3+} indicates the reaction of nitric oxide and oxygen is the rate-limiting step. The reaction cycle is completed with the final products of NO_3^- (4.5 mM) and Fe^{3+} (0.1 M) in the solution.

Conclusion

This research has focused on the elucidation of the reaction mechanisms involved in the oxidation of ferrous ion to ferric ion using oxygen and a low-concentration nitrite present in a sulfuric-acid electrolyte.

REFERENCES

1. G.E. Kingsley, US Patent 914730 (1909).
2. H.D. Rankin, US Patent 1150787 (1915).
3. E. Pauling, *Metall. Erz.*, **35**, 451 (1940).
4. F. Habashi, *Society of Mining Engineers, AIME*, **254**, 224 (1973).
5. G. Bjorling and G.A. Kolta, *J. Chem.*, **9**, 187 (1966).
6. F. Caldon, US Patent 4084961 (1978).
7. H.M. Brennecke, O. Bergmann, R.R. Ellefson, D.S. Davies, R.E. Leuders and R.A. Spitz, *J. Min. Eng.*, **12**, 20 (1981).
8. G. Van Weert, K.J. Fair and J.C. Schneider, 116th Annual TMS/AIME Meeting (1986).
9. M.J.V. Beattie, R. Randsepp and A. Ismay, *Proc. Intern. Symp, Oxford*, **1**, 431 (1989).
10. C.G. Anderson, L.E. Krys and K.D. Harrison, US Patent 5096486 (1992).
11. C.G. Anderson, K.D. Harrison and L.E. Krys, *Prec. Met., IPMI Con.*, 19 (1993).
12. S.A. Baldwin and G.V. Van Weert, *Hydrometallurgy*, **42**, 209 (1996).
13. C.G. Anderson, *J. Met.*, **55**, 32 (2003).
14. E. Abel, H. Schmid and F. Pollak, *Monatsh. Chem.*, **69**, 125 (1936).
15. E. Abel and H. Schmid, *Z. Phys. Chem.*, **132**, 56 (1928).
16. I.R. Epstein, K. Kustin and R.H. Simoyi, *J. Am. Chem. Soc.*, **104**, 712 (1982).
17. D. Thomas and J. Vanderschuren, *Ind. Eng. Chem. Res.*, **36**, 3315 (1997).
18. A.R. Butler and J.H. Ridd, *Nitric Oxide*, **10**, 20 (2004).
19. J.Y. Park and Y.N. Lee, *J. Phys. Chem.*, **92**, 6294 (1988).
20. C.A. Bunton and G. Stedman, *J. Chem. Soc.*, **3**, 3466 (1959).
21. G.Y. Markovitz, S.E. Schwartz and L. Newman, *Inorg. Chem.*, **20**, 445 (1981)
22. M.P. Pradhan, N.J. Suchak, P.R. Walse and J.B. Joshi, *Chem. Eng. Sci.*, **52**, 4569 (1997).
23. Y. Kameoka and R.L. Pigford, *Ind. Eng. Chem. Fundam.*, **16**, 163 (1977).
24. M.P. Pradhan and J.B. Joshi, *AIChE J.*, **45**, 38 (1999).
25. H.H. Awad and D.M. Stanbury, *Int. J. Chem. Kin.*, **25**, 375 (1993).
26. B.D. Beake, J. Constantine and R.B. Moodie, *J. Chem. Soc.*, 1653 (1992).
27. O. Gok, *Nitric Oxide*, **25**, 47 (2011).